Available online at www.sciencedirect.com
SCIENCE DIRECT®
Coordination Chemistry Reviews 241 (2003) 47–60
COORDINATION CHEMISTRY REVIEWS
www.elsevier.com/locate/ccr

# Structural aspects of copper(I) and silver(I) sulfide clusters of pentamethylcyclopentadienyl trisulfido tungsten(VI) and molybdenum(VI)

Jian-Ping Lang [a,*], Shun-Jun Ji [a], Qing-Feng Xu [a], Qi Shen [a], Kazuyuki Tatsumi [b]

[a] Department of Chemistry and Chemical Engineering, Suzhou University, 1 Shizi Street, Suzhou 215006, Jangsu, People's Republic of China
[b] Research Center for Materials Science, Department of Chemistry, Graduate School of Science, Nagoya University, Furo-cho, Chikusa-ku, Nagoya 462-8602, Japan

Received 8 February 2002; accepted 21 November 2002

**Contents**



**Abstract**

The use of mononuclear metal sulfide ligands to construct heterometallic sulfide clusters is an area of inorganic chemistry that has received ever-increasing attention in recent years. This article reviews the advances that have been made in the synthesis and coordination chemistry of organometallic trithio complex, $[PPh_4][(\eta^5\text{-}C_5Me_5)MS_3]$ (M = W, Mo). From a set of 24 W(Mo) | Cu(Ag, Au, Pd) | S clusters containing $(\eta^5\text{-}C_5Me_5)MS_3$ moiety, three basic cluster fragments along with a rare fragment are topologically outlined. Each specific structure is briefly discussed and particular emphasis is put upon how the specific cluster array is assembled via these fragments or their certain combination is highlighted.


*Keywords:* Pentamethylcyclomethyldineyl trisulfido tungsten(VI) and molybdenum(VI); Synthesis; Cluster fragments; Copper(I) cluster; Silver(I) cluster

## 1. Introduction

Synthesis of transition metal sulfide clusters continues to be a major objective in inorganic chemistry [1–15]. Use of thiometallates is a popular method for prepara-

* Corresponding author. Tel.: +86-512-6521-3506; fax: +86-512-6522-4783
*E-mail address:* jplang@suda.edu.cn (J.-P. Lang).

0010-8545/02/$ - see front matter © 2002 Elsevier Science B.V. All rights reserved.
PII: S0010-8545(02)00309-0

tion of metal sulfide clusters with various nuclearity, and in particular thiotungstates and thiomolybdates have served as key building blocks for a wide variety of homo- and hetero-metallic sulfide clusters. The clusters obtained from these precursors have shown rich chemistry of their own [16–27], and may be relevant to biological systems [27–32], industrially important catalysis [33–37], and optoelectronic materials [38–42]. On the other hand, we have succeeded in the synthesis of a series of organometallic trisulfido complexes $[(\eta^5\text{-}C_5Me_5)MS_3Li_2(THF)_2]_2$ (M = Nb [43], Ta [44]) and $[(\eta^5\text{-}C_5Me_5)MS_3]^-$ (M = W [45], Mo [46]). The niobium and tantalum complexes were obtained from reactions of $[(\eta^5\text{-}C_5Me_5)MCl_4]$ with $Li_2S_2$ in THF, and the lithium cations were readily replaced by late transition metals, forming heterometallic sulfido clusters [47]. However, the tungsten and molybdenum complexes were isolated from reactions of $[(\eta^5\text{-}C_5Me_5)MCl_4]$ with thiolates followed by C–S bond-cleaving reactions of thiolates, and exhibited high reactivity toward alkynes to afford 1,2-enedithiolates [46]. Having noted that these trisulfido complexes may be viewed as derivatives of tetrathiometallates and can serve as potential building blocks for heterometallic sulfide clusters, we have examined the reactions of these anions, especially those of tungsten and molybdenum, with transition metals such as copper(I), silver(I), etc. Indeed, a new family of Mo(W) | Cu(Ag) | S clusters has been generated therefrom, many of which exhibit unusual cluster frameworks [48–56]. In this review we focus on the synthesis and coordination chemistry of the clusters containing the $(\eta^5\text{-}C_5Me_5)MS_3$ (M = W, Mo) moiety we have isolated so far, and if necessary, compare their chemistry with those of $[MES_3]^{2-}$ (M = W, Mo; E = O, S) species.

## 2. Synthesis of $[PPh_4][(\eta^5\text{-}C_5Me_5)MS_3]$ (M = W, Mo)

In 1993, Geoffroy et al. reported that the reaction of $[(\eta^5\text{-}C_5Me_5)WCl_4]$ with $H_2S$ in the presence of $NEt_3$ produced a small amount of the trithio complex $[NEt_3H][(\eta^5\text{-}C_5Me_5)WS_3]$ along with *anti*-$[(\eta^5\text{-}C_5Me_5)WS_2]_2$, $[(\eta^5\text{-}C_5Me_5)_2W_2S_2(S_2)_2]$, and $[NEt_3H][(\eta^5\text{-}C_5Me_5)WOS_2]$ [57]. As shown in Scheme 1, we found other better routes to isolate, in 83% yield, rather pure $[PPh_4][(\eta^5\text{-}C_5Me_5)MS_3]$ (M = W, **1**; M = Mo, **2**) [45,46]. A facile C–S bond cleavage reaction is believed to occur during the reaction of $[(\eta^5\text{-}C_5Me_5)WCl_4]$ with $Li_2edt$. The synthesis of the molybdenum analogue $[PPh_4][(\eta^5\text{-}C_5Me_5)MoS_3]$ (**2**) is not so straightforward. Therefore, another route was 'designed' to isolate it in pure form, Scheme 2. Reactions of $[(\eta^5\text{-}C_5Me_5)MoCl_4]$ with $LiS^tBu$ in THF afforded $[(\eta^5\text{-}C_5Me_5)Mo(S^tBu)_3]$ in a rather high yield. Addition of 1/4 equiv. of $S_8$ to $[(\eta^5\text{-}C_5Me_5)Mo(S^tBu)_3]$ in THF formed a dark green solution, which may contain a mixture of $[(\eta^5\text{-}C_5Me_5)MoS_2(S^tBu)]$, $[(\eta^5\text{-}C_5Me_5)MoOS(S^tBu)]$, *anti*-$[(\eta^5\text{-}C_5Me_5)MoS_2]_2$ and an unidentified green compound. On further treatment with excess $Li_2S_2$, subsequent purification produced dark red compound **2** in 40–60% yield. X-ray analysis of **1** and **2** confirmed that the $[(\eta^5\text{-}C_5Me_5)MS_3]^-$ anion has a three-legged piano stool structure with the $S_3$ plane parallel to the $(\eta^5\text{-}C_5Me_5)$ ring. The mean W=S and Mo=S bond lengths, 2.192 and 2.188 Å, are longer than those of $(NH_4)_2[WS_4]$ (2.177 Å)and $(NH_4)_2[MoS_4]$ (2.178 Å) [16]. The steric bulkiness and electron-donor character of $\eta^5\text{-}C_5Me_5$ may contribute to this unusual trend.

## 3. Synthesis of copper or silver clusters containing $[(\eta^5\text{-}C_5Me_5)MS_3]^-$ (M = W, Mo) moiety

As shown in Scheme 3, the $(\eta^5\text{-}C_5Me_5)MS_3$ moiety has a pyramidalized geometry with three S–S edges. When one M′, two M′, and three M′ atoms (M′ = Cu(I) or Ag(I)) are bound to these S–S edges in a stepwise manner, three basic cluster fragments, $[(\eta^5\text{-}C_5Me_5)MS_3M']$ (**a**), $[(\eta^5\text{-}C_5Me_5)MS_3M']$ (**b**), and $[(\eta^5\text{-}C_5Me_5)MS_3M']$ (**c**), are formed. Therefore, if the ratio between $[PPh_4][(\eta^5\text{-}C_5Me_5)MS_3]$ and M′ salt is carefully controlled, clusters with fragments **a**, **b** and **c** can be isolated, respectively. Examples are $[(\eta^5\text{-}C_5Me_5)WS_3Au(PPh_3)]$, $[(\eta^5\text{-}C_5Me_5)WS_3(CuPPh_3)_2Br]$, and $[(\eta^5\text{-}C_5Me_5)WS_3Cu_3(PPh_3)_3(NO_3)](NO_3)$ [48,52,55]. Fragments **a** and **b** possess terminal S and/or doubly-bridging S atoms, which may further bind more M′ atoms during

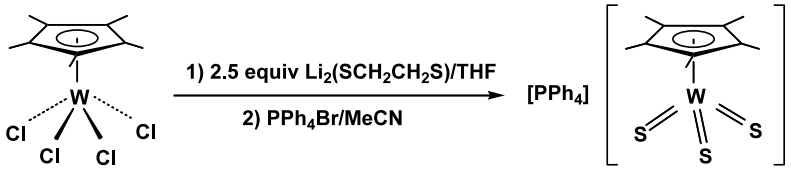


(1)

orange-red crystals

82 % yield

Scheme 1.

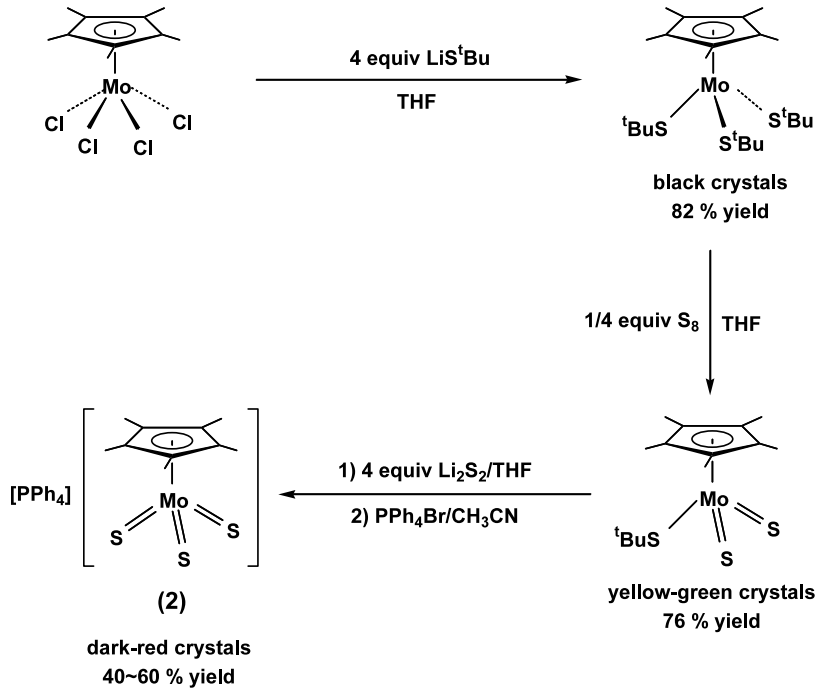


Scheme 2.

the reaction. Thus clusters with mixed fragments such as $[\{(\eta^5\text{-}C_5Me_5)WS_3\}_2Ag_3(PPh_3)_3](NO_3)$ and $[\{(\eta^5\text{-}C_5Me_5)WS_3\}_3Cu_7(MeCN)_9](PF_6)_4$ have been observed [52,56]. Furthermore, some preformed clusters are good precursors to generate new types of clusters. For example, $[PPh_4]_2[(\eta^5\text{-}C_5Me_5)WS_3(CuBr)_3]_2$ [48] reacts with excess $Li_2S_2$ to form $[PPh_4][\{(\eta^5\text{-}C_5Me_5)WS_3\text{-}Cu_2\}_3S_2]$ [51]. In addition, it is also possible that only one sulfur of the $(\eta^5\text{-}C_5Me_5)MS_3$ moiety coordinates one M′ center, forming a rare cluster fragment (**d**), which was observed when $HgCl_2$ reacts with $(\eta^5\text{-}C_5Me_5)WS_3$ moiety [58]. So far, a total of 24 W(Mo) | Cu(Ag, Au, Pd, Hg) | S clusters containing $(\eta^5\text{-}C_5Me_5)MS_3$ moiety (**3**–**26**) have been prepared and structurally characterized. More than ten types of cluster skeletal structures have been confirmed, most of which consist of each of the three cluster fragments or certain combination of these fragments.

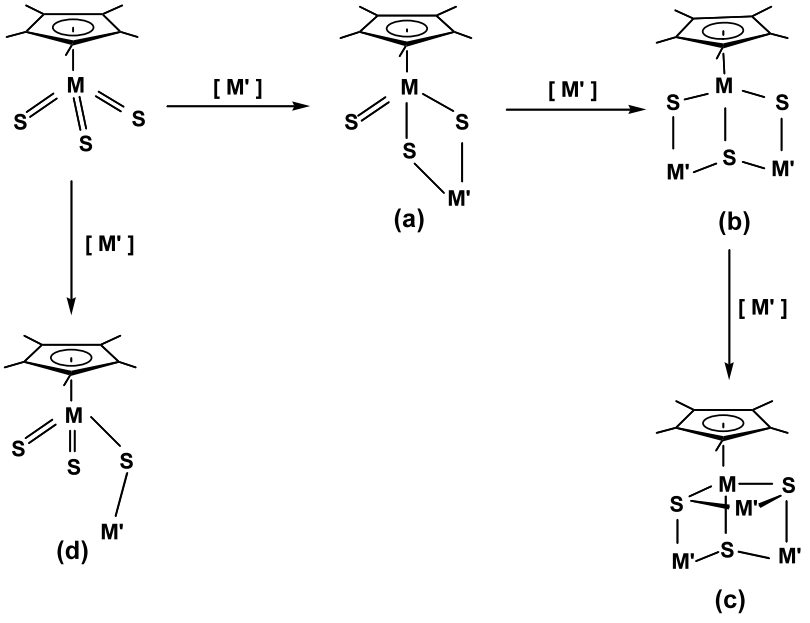


Scheme 3.

## 4. Specific cluster structures

According to the ratio of M and M′ in these 24 compounds, they are classified into nine categories: MM′, $MM'_2$, $MM'_3$, $M_2M'$, $M_2M'$, $M_2M'$, $M_3M'_6$, $M_3M'_7$ and $M_4M'_4$; we briefly discuss their synthesis and important structural features in the following subsections.

### 4.1. MM′-type clusters

There are only two compounds available: [($\eta^5$-$C_5Me_5$)$WS_3$Au($PPh_3$)] (**3**) and [($\eta^5$-$C_5Me_5$)$WS_3$Pd(dppe)]Cl (**4**). The facile reactions of **1** with equimolar [AuCl($PPh_3$)] or [$PdCl_2$(dppe)] in MeCN afforded **3** and **4** in very good yield [52]. Both the molecular structure of **3** and the structure of the cation of **4** contains a ($\eta^5$-$C_5Me_5$)$WS_3$M′ fragment (**a**), i.e. one [($\eta^5$-$C_5Me_5$)$WS_3$] moiety binds one Au(I) or Pd(II) through two S atoms to form a dinuclear structure with a four-membered M($\mu_2$-S)M′ ring. The coordination geometry of the Au atom adopts exactly trigonal-planar (Fig. 1), and the observed W–Au distance of 2.8279(5) Å is close to those of [$WS_4$($AuCH_2PPh_3$)$_2$] (2.820(2) Å) [59] and [$WS_4$(Au($PPh_2CH_3$)$_2$] (2.840(1) Å) [60]. On the other hand, Pd(II) is tetrahedrally coordinated by two $\mu_2$-S and two P atoms of the dppe ligand (Fig. 2), and the W–Pd distance of 2.9042(8) Å is slightly longer than [$WS_4$Pd(dppe)] [61] and [$WS_4${Pd(allyl)}$_2$] [62]. So far, no similar copper or silver analogues have been isolated.

### 4.2. $MM'_2$-type clusters

Four compounds have been reported: [($\eta^5$-$C_5Me_5$)$WS_3$(M′$PPh_3$)$_2$Br] (**5**: M′ = Cu; **6**: M′ = Ag), [$PPh_4$][($\eta^5$-$C_5Me_5$)$WS_3$(CuCN)$_2$] (**7**), and [($\eta^5$-$C_5Me_5$)$WS_3Ag_2X$]$_\infty$ (**8**: X = Br; **9**: X = CN).

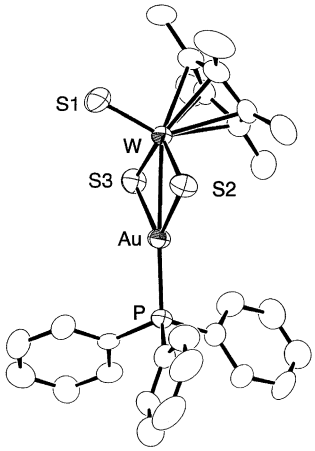


Fig. 1. Molecular structure of [($\eta^5$-$C_5Me_5$)$WS_3$Au($PPh_3$)] (**3**) with 50% thermal ellipsoids. Hydrogen atoms are omitted for clarity. Reproduced with permission from Ref. [52].

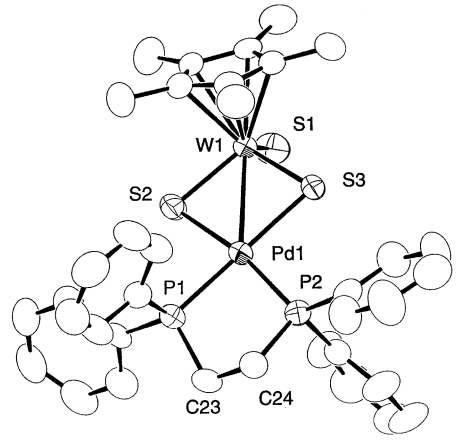


Fig. 2. Structure of the cation of [($\eta^5$-$C_5Me_5$)$WS_3$Pd(dppe)]Cl (**4**) with 50% thermal ellipsoids. Hydrogen atoms are omitted for clarity. Reproduced with permission from Ref. [52].

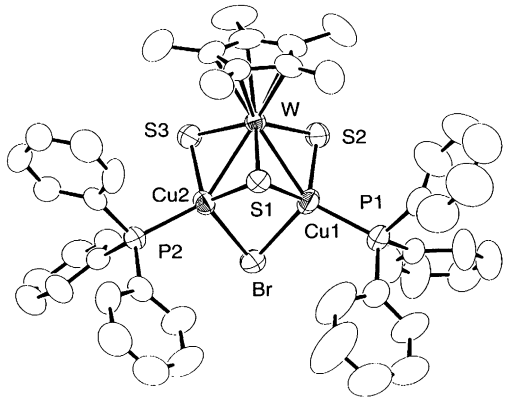


Fig. 3. Molecular structure of [($\eta^5$-$C_5Me_5$)$WS_3Cu_2$($PPh_3$)$_2$Br] (**5**) with 50% thermal ellipsoids. Hydrogen atoms are omitted for clarity. Reproduced with permission from Ref. [55].

Compound **5** was obtained from the reaction of **1** with 2 equiv. of CuBr and excess $PPh_3$ in $CHCl_3$ [55] while **6** was isolated from the reaction of **8** with excess $PPh_3$ in $CHCl_3$ [49]. As **5** and **6** are isomorphous and their structures are very similar, only the structure of **5** is shown in Fig. 3. They all have a butterfly-shaped ($\eta^5$-$C_5Me_5$)$WS_3M'_2$ fragment (**b**) where two M′ (M′ = Cu or Ag) atoms are bound to the ($\eta^5$-$C_5Me_5$)$WS_3$ moiety across two S–S edges with an acute angle M′–W–M′ = 64.18(4)° (**5**) or 61.52(2)° (**6**). A bromide further bridges the two M′ atoms with a small angle of M′(1)–$\mu_2$-Br–M′(2) = 66° (**5**) and 70° (**6**). However, the bridging bromide moves out of the triangular face of M′(1), S(1) and M′(2). The seven-atom [$WS_3M'_2$Br] cluster geometry in **5** and **6** may be regarded as an intermediate between the six-atom [$WS_3M'_2$] skeleton in [$WOS_3M'_2$($PPh_3$)$_3$] [63–65] and the eight-atom cubane structure of [$WS_3M'_3$Br] in [$WS_3M'_3$($PPh_3$)$_3$Br] (M′ = Cu [66], M′ = Ag [67]). Each M′ atom in **5** and **6** is bound to two sulfides, one bromide, and one $PPh_3$ ligand, forming a distorted tetrahedral coordination geometry. The

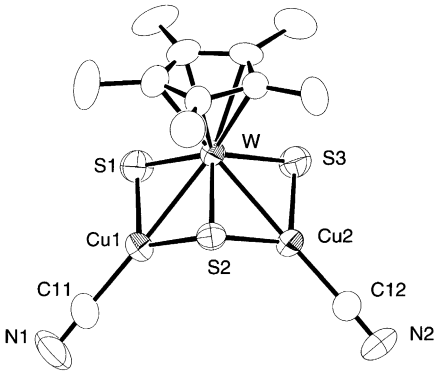


Fig. 4. Structure of the anion of $[PPh_4][(\eta^5\text{-}C_5Me_5)WS_3(CuCN)_2]$ (**7**) with 50% thermal ellipsoids. Hydrogen atoms are omitted for clarity [58].

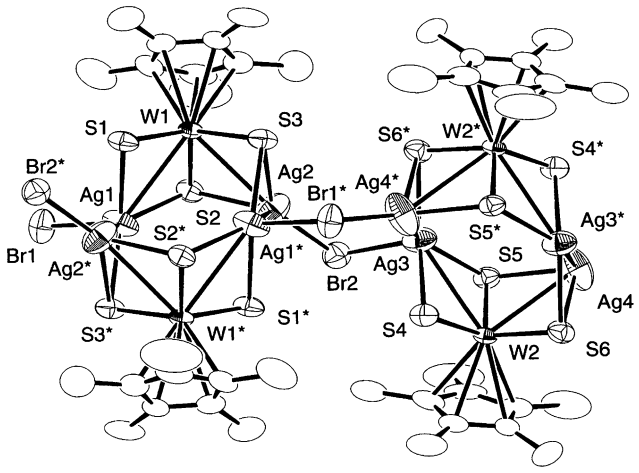


Fig. 6. Structure of a repeating unit of **8** with 50% thermal ellipsoids. Hydrogen atoms are omitted for clarity. Reproduced with permission from Ref. [49].

average W–Cu and W–Ag bond lengths, 2.704(1), 3.0483(5) Å, are comparable to those in $[WOS_3M'_2(PPh_3)_3]$ [63–65] and $[WS_4M'_3(PPh_3)_3Br]$ ($M' = Cu$ [66], $M' = Ag$ [67]).

Treatment of an acetonitrile solution of **1** in MeCN with 2 equiv. of CuCN led to the formation of red crystals of **7** [58]. The structure of the anion of **7** also contains a similar $(\eta^5\text{-}C_5Me_5)WS_3Cu_2$ fragment (**b**). However, each copper adopts a typical trigonal-planar coordination geometry with one CN and two S atoms. Therefore, the average W–Cu length of 2.6539(8) is shorter than that of **5**. The Cu(1)–$\mu_3$-S–Cu(2) bond angle of 97.47(6)° is remarkably larger than the corresponding one of **5** (78.05(8)°) (Fig. 4).

Reactions of **1** with 3 equiv. of AgBr or AgCN in MeCN instantly gave rise to dark red products of **8** or **9** in nearly quantitative yield [49,54]. Compounds **8** and **9** have a very similar chemical formula. However, they display a completely different polymeric chain structure in the solid state. As shown in Fig. 5, **8** possesses an unusual ladder-shaped one-dimensional chain structure. The geometries of two crystallographically independent $[(\eta^5\text{-}C_5Me_5)WS_3]_2Ag_4$ clusters in the chain are practically identical, and an inversion center resides in the middle of each cluster core (Fig. 6). The repeating unit $[\{(\eta^5\text{-}C_5Me_5)WS_3\}_2Ag_4Br_2]$ in **8** could be regarded as built up of two $(\eta^5\text{-}C_5Me_5)WS_3Ag_2$ fragments (**b**) via additional Ag–S (e.g. Ag(1)–S(3*) and Ag(1*)–S(3); Ag(3)–S(6*) and Ag(3*)–S(6)) and Ag–Ag (e.g. Ag(1)–Ag(2*) and Ag(2)–Ag(1*); Ag(3)–Ag(4*) and Ag(3*)–Ag(4)) interactions. The Ag(1)–Ag(2*) and Ag(3)–Ag(4*) distances of 2.916(2) and 2.895(2) Å are shorter than those in $[(PPh_3)_4Ag_4(mt)_4]$ (3.089(2)–3.110(1) Å, mt = 2-mercaptothiazoline) [68] and $[\{Ag(2\text{-}Me_3SiC_6H_4S)\}_4]_2$ (3.065(4)–3.320(5) Å) [69], which indicates the presence of weak interactions between the Ag atoms. Within the cluster, the Ag(1) atom (or Ag(3)) bridges two sulfur atoms of one $(\eta^5\text{-}C_5Me_5)WS_3$ moiety, and is also bound to a sulfur atom of the other $(\eta^5\text{-}C_5Me_5)WS_3$ moiety, resulting in a distorted tetrahedral $AgS_3Br$ coordination geometry. On the other hand, Ag(2) (or (Ag(4)) assumes an ca. trigonal-planar geometry with two S atoms of a $(\eta^5\text{-}C_5Me_5)WS_3$ moiety and a Br bridge. The mean W–Ag length of 3.005(2) Å is comparable to those found in $[Nd(DMF)_8]_n[W_4S_{16}Ag_4]_n$ (2.964(2) Å) [70] and $[\gamma\text{-}MePyH]_n[WS_4Ag]_n$ (2.971(2) Å) [71]. We compare the core geometry of $[\{(\eta^5\text{-}C_5Me_5)WS_3\}_2Ag_4Br_2]$ in **8** with the geometry of the closely related compounds $[(MS_4)_2Ag_4(PPh_3)_4]$ (M = Mo, W) [72,73]. The $M_2S_6Ag_4$ skeleton of the latter cluster is hexagonal prismatic, while in the former cluster unit, two Ag–S bonds, Ag(1)–S(1) and Ag(1*)–S(1*) (or Ag(4)–S(4)

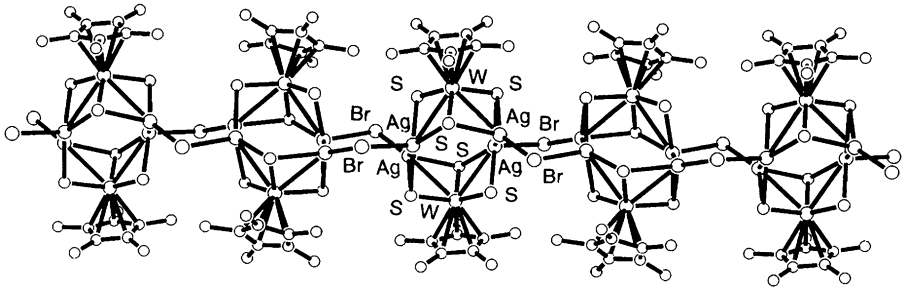


Fig. 5. Ladder-shaped 1D structure of $[(\eta^5\text{-}C_5Me_5)WS_3Ag_2Br]_\infty$ (**8**). Reproduced with permission from Ref. [49].

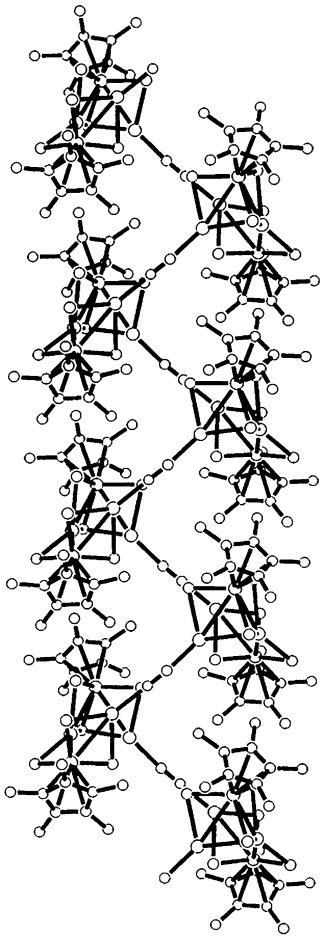

Fig. 7. Extended structure of $[(\eta^5\text{-}C_5Me_5)WS_3Ag_2CN]_\infty$ (**9**) looking down the $c$-axis. Reproduced with permission from Ref. [54].

and Ag(4*)–S(4*), are broken. The difference may arise from the steric hindrance occurring between adjacent $\eta^5$-$C_5Me_5$ rings and bromides in the polymeric structure of **8**.

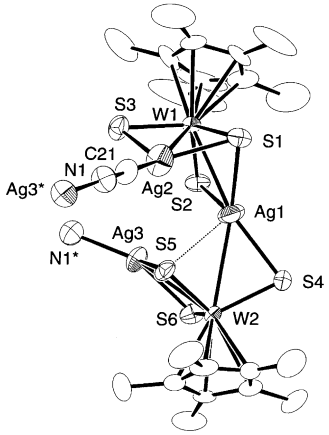


Fig. 8. Structure of the repeating unit of **9** with 50% thermal ellipsoids. Hydrogen atoms are omitted for clarity. Reproduced with permission from Ref. [54].

On the other hand, the one-dimensional chain backbone of **9** is made of pentanuclear $\{[(\eta^5\text{-}C_5Me_5)WS_3]_2Ag_3\}$ clusters and μ-CN anions (Fig. 7). Each CN links two clusters through interactions with Ag(2) of one cluster and Ag(3*) of another, forming an intriguing helical array of the repeating $\{[(\eta^5\text{-}C_5Me_5)WS_3]_2Ag_3(CN)\}$ units. Because **9** crystallizes in a centrosymmetric space group $P2_1/c$, there are two helical strands with opposite chirality in a unit cell. The Ag–CN–Ag portion is practically linear, with the Ag(2)–C(21)–N(1) and C(21)–N(1)–Ag(3*) angles being 173(1) and 179(1)°, respectively. The structure of the repeating pentanuclear cluster unit is shown in Fig. 8. This cluster is made of two $(\eta^5\text{-}C_5Me_5)WS_3Ag$ fragments (**a**) that are connected by Ag(1). Alternatively, it may be visualized as a combination of a $(\eta^5\text{-}C_5Me_5)WS_3Ag$ fragment (**a**) and a $(\eta^5\text{-}C_5Me_5)WS_3Ag_2$ fragment (**b**) through the interaction between Ag(1) and S(4). Coordination of S atoms at Ag(1) occurs in an asymmetric way. Bonding with the three sulfur atoms, S(1), S(2), and S(4), is relatively strong, forming a slightly pyramidalized Y-shape coordination geometry. In addition, we noticed a weak interaction between Ag(1) and S(5) (2.81 Å). Because of the unsymmetrical coordination environment at Ag, W–S bond lengths also vary substantially from 2.185(4) to 2.321(4) Å. The mean W–Ag distance (2.952 Å) is not unusual as compared with those of **8**. Although CN-bridged metal polymers are ubiquitous, those having helical chain structures are very rare. Examples are $[(OC)Pd(\mu\text{-}CN)Mn(\eta\text{-}C_5H_4Me)(CO)_2]_4$ (orthogonal arrangement of helical units) [74] and K[Cu(μ-CN)(CN)] (spiral chain) [75].

### 4.3. $MM_3'$-type clusters

Clusters belonging to this group include: $[(\eta^5\text{-}C_5Me_5)MS_3Cu_3(EPh_3)_2Br_2]$ (**10**: M = Mo, E = P; **11**: M = W, E = P; **12**: M = W, E = As), $[PPh_4][(\eta^5\text{-}C_5Me_5)WS_3Cu_3Br_3(dppm)]$ (**13**); $[(\eta^5\text{-}C_5Me_5)WS_3\text{-}Cu_3(PPh_3)_3(NO_3)](NO_3)$ (**14**); $[(\eta^5\text{-}C_5Me_5)WS_3\text{-}$

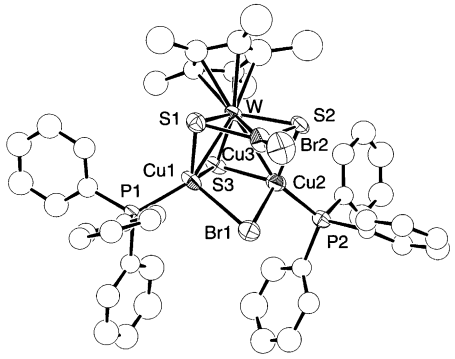


Fig. 9. Molecular structure of $[(\eta^5\text{-}C_5Me_5)WS_3Cu_3(PPh_3)_3Br]$ (**11**) with 50% thermal ellipsoids. Hydrogen atoms are omitted for clarity. Reproduced with permission from Ref. [53].

$Cu_3(PPh_3)_3Cl](PF_6)$ (**15**), $[(\eta^5\text{-}C_5Me_5)WS_3Cu_3Cl(MeCN)(pz)]_\infty(PF_6)_\infty$ (**16**).

Treatment of $[PPh_4]_2[(\eta^5\text{-}C_5Me_5)WS_3(CuBr)_3]_2$ (**21**) [48] with excess $AsPh_3$, $PPh_3$, and dppm in MeCN led to the formation of **10**–**13** in good yield [53]. Since **10**–**12** are isomorphous, only the structure of **11** was determined. As shown in Fig. 9, the main structural feature of **11** resembles that of $[NEt_4]_3[WOS_3Cu_3Br_4] \cdot 2H_2O$ [76], and consists of a distorted $WS_3Cu_3Br$ cube where the Cu(3)–Br(1) bond is broken. Alternatively, it can be described as having an incomplete $(\eta^5\text{-}C_5Me_5)WS_3Cu_3$ fragment (**c**) with a $\mu_2$-Br(1) linking Cu(1) and Cu(2) atoms. The Cu(3) atom assumes a trigonal-planar geometry, coordinated by one terminal Br and two $\mu_3$-S atoms. On the other hand, Cu(1) and Cu(2) atoms have a distorted tetrahedral geometry, coordinated by one $\mu_2$-Br, one P($PPh_3$), and two $\mu_3$-S atoms. Because of the different coordination geometry, the W–Cu(3) distance of 2.674(2) Å is 0.03 Å shorter than the average of the W–Cu(1) and W–Cu(2) distances. In comparing the core structure with that of **5** note that formally, the structure of **11** is made by addition of one CuBr group to the cluster framework of **5**. Similar to that discussed in **5** or **6**, the bridging Br(1) atom moves out of the plane of Cu(1), S(3), and Cu(2), tilting away from the Cu(3) atom. This results in a very long Cu(3)···Br(1) distance of 3.15 Å and an acute Cu(1)–Br(1)–Cu(2) angle of 68.03(7)°.

Similar to **11**, the structure of the anion of **13** also consists of an incomplete $(\eta^5\text{-}C_5Me_5)WS_3Cu_3$ fragment (**c**) and may be envisaged as a dppm adduct of $[PPh_4][(\eta^5\text{-}C_5Me_5)WS_3(CuBr)_3]$ (Fig. 10). There are three CuBr groups, and two of them are bridged by a dppm ligand. Therefore, the Cu(1) atom has a trigonal-planar geometry, coordinated by one terminal Br and two $\mu_3$-S atoms, while the Cu(2) and Cu(3) atoms have a distorted tetrahedral geometry, coordinated by one terminal Br, one P(dppm), and two $\mu_3$-S atoms. Again, because of the different copper coordination geometries, the W–Cu(3) distance of 2.6387 Å is 0.14 Å shorter than the mean distance of W–Cu(1) and W–Cu(2). A notable difference between the structures of **11** and **13** is that, in the former structure, the Cu(1) and Cu(2) atoms are bridged by a Br atom, while in the latter structure, a dppm ligand links the Cu(1) and Cu(2) atoms. The Cu–S(1)–Cu(2) bond angle of 100.28(6)° in **13** is 19° larger than the corresponding angle (Cu(1)–S(3)–Cu(2)) in **11**.

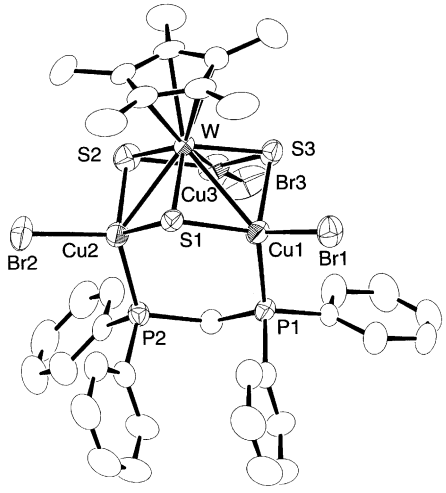


Fig. 10. Structure of the anion of $[PPh_4][(\eta^5\text{-}C_5Me_5)WS_3Cu_3Br_3(dppm)]$ (**13**) with 50% thermal ellipsoids. Hydrogen atoms are omitted for clarity. Reproduced with permission from Ref. [53].

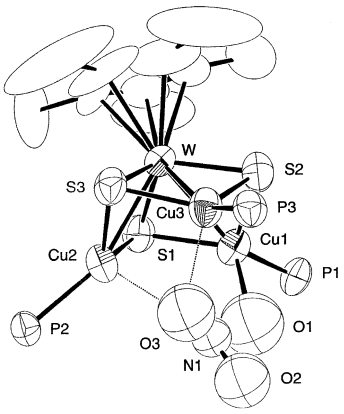


Fig. 11. Structure of the cation of $[(\eta^5\text{-}C_5Me_5)WS_3Cu_3(PPh_3)_3(NO_3)](NO_3)$ (**14**) with 50% thermal ellipsoids. Phenyl groups and hydrogen atoms are omitted for clarity. Reproduced with permission from Ref. [52].

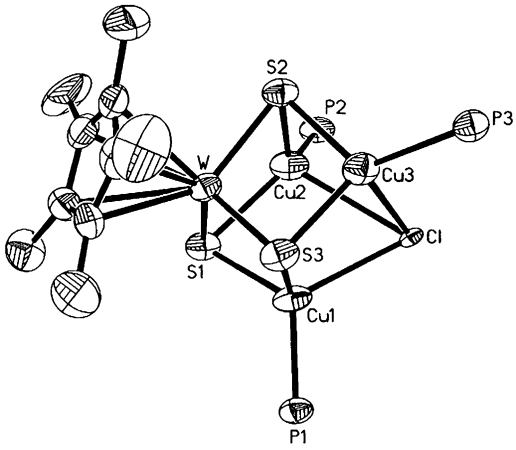


Fig. 12. Structure of the cation of $[(\eta^5\text{-}C_5Me_5)WS_3Cu_3(PPh_3)_3Cl](PF_6)$ (**15**) with 50% thermal ellipsoids. Phenyl groups and hydrogen atoms are omitted for clarity. Reproduced with permission from Ref. [58].

Compounds **14**–**15** were isolated from reactions of **1** with either $[Cu(PPh_3)_2NO_3]$ or $[Cu(MeCN)_4](PF_6)/PPh_3$/LiCl in MeCN [52,58]. As shown in Figs. 11 and 12, X-ray analysis confirmed that both of them have almost the same incomplete $(\eta^5\text{-}C_5Me_5)WS_3Cu_3$ fragment (**c**), and a $PPh_3$ ligand is coordinated at each Cu site. Interestingly, the void of the incomplete cube of **14** or **15** is filled by a $NO_3$ group or Cl in two different ways.

In the structure of the cation of **14**, one $NO_3$ anion is strongly bound to Cu(1) (Cu(1)–O(1) = 2.25(2) Å), and weakly interacts with Cu(2) and Cu(3) through O(3), with the distances of 2.60 and 2.43 Å. Due to the interactions with nitrate oxygen atoms, three copper atoms distort from a trigonal-planar to tetrahedral coordination geometry by varying degrees. Although the W–Cu(1) bond length of 2.716(2) Å is normal, the W–Cu(2) and W–Cu(3) lengths, 2.693(2) and 2.688(2) Å, are somewhat longer than those containing three-coordinated Cu clusters such as **11** and **13**. However, in the cation of **15**, a Cl atom directly fills on the void of the $WS_3Cu_3$ incomplete cube with three long Cu–Cl distances (mean value = 2.698 Å), forming a strongly distorted cubane structure. The resulting $WS_3Cu_3Cl$ cube is closely related to those of neutral clusters $[WES_3Cu_3(PPh_3)_3Cl]$ (E = O, S) [77]. The three Cu atoms are not equivalent, and their coordination variability ranges from a strongly distorted tetrahedron (Cu(1) and Cu(3)) to a nearly trigonal-planar coordination (Cu(2)) with a long Cu(2)–Cl interaction (2.746(2) Å). Because of the different coordination geometries of the copper atoms, the W–Cu(2) distance of 2.6967(14) Å is shorter than the mean distance of W–Cu(1) and W–Cu(2) bonds (2.7429(13) and 2.8859(15) Å).

The last member (**16**) of this group was obtained by treatment of $[\{(\eta^5\text{-}C_5Me_5)WS_3\}_3Cu_7(MeCN)_9](PF_6)_4$ (**24**) with pyrazine (pz) in MeCN in the presence of LiCl [56]. Figs. 13 and 14 display its two-dimensional sheet structure, and the repeating unit of the 2D network and connectivity. The repeating cluster $[(\eta^5\text{-}C_5Me_5)WS_3Cu_3(MeCN)]$ also contains an incomplete

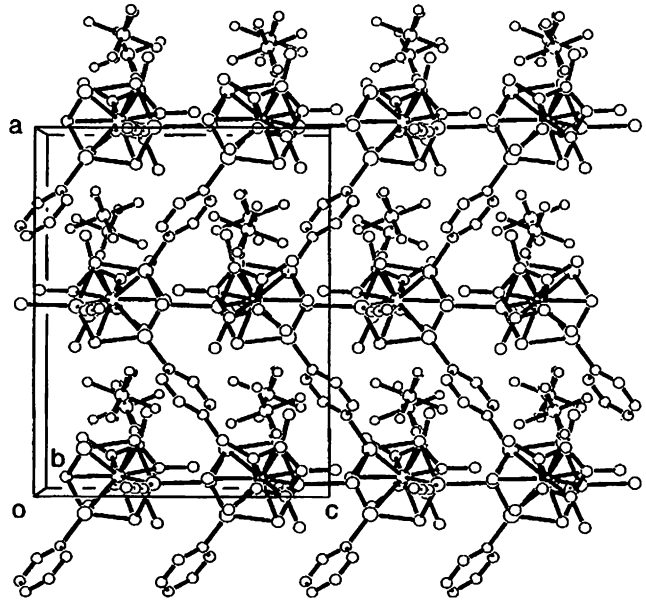


Fig. 13. Extended 2D layer structure of $[(\eta^5\text{-}C_5Me_5)WS_3Cu_3(CH_3CN)Cl(pz)]_\infty(PF_6)_\infty$ (**16**) looking down the *b*-axis. Reproduced with permission from Ref. [56].

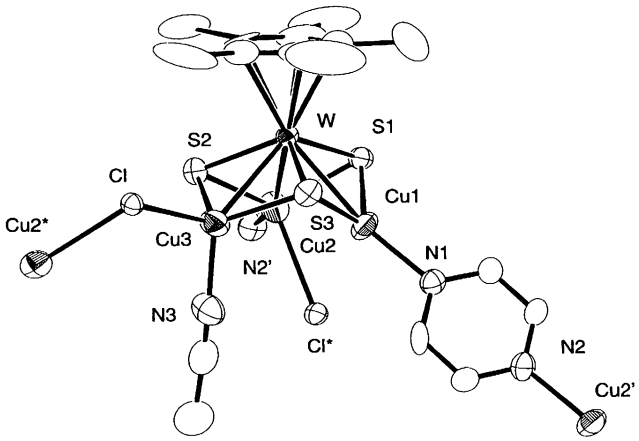


Fig. 14. Structure of a repeating unit of **16** with 50% thermal ellipsoids. Hydrogen atoms are omitted for clarity. Reproduced with permission from Ref. [56].

$(\eta^5\text{-}C_5Me_5)WS_3Cu_3$ fragment (**c**), which closely resembles those of **11**, **13**, **14**, and **15**. It is interconnected by pyrazine through interactions with Cu(1) and Cu(2′), to form zigzag chains extending along the *a* axis where the orientation of the $[(\eta^5\text{-}C_5Me_5)WS_3Cu_3(MeCN)]$ unit is alternating. The chains are then connected by $\mu_2$-Cl at Cu(2*) and Cu(3) along the *c* axis. The resulting 2D network forms a parallelogrammic mesh, and each cavity is filled by a $PF_6^-$ anion. The surfaces of each layer are covered with $(\eta^5\text{-}C_5Me_5)WS_3$ rings, and the thickness of the layers is estimated to be ca. 9.9 Å. The layers are separated by ca. 3.5 Å, and no inter-layer bonding interactions are observed. Cu(1) is coordinated by N(pz) and two $\mu_3$-S atoms, and the W–Cu(1) distance is relatively short (2.654(2) Å). On the other hand, the Cu(2) and Cu(3) are coordinated by N (pz or MeCN), $\mu_2$-Cl and two $\mu_2$-S atom, and the W–Cu interactions are slightly weaker (2.673(2) and 2.722(2) Å).

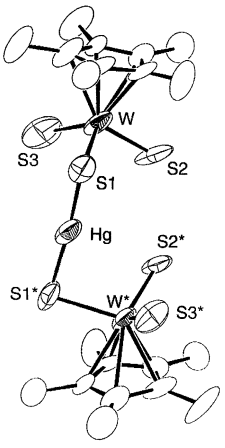


Fig. 15. Molecular structure of $[\{(\eta^5\text{-}C_5Me_5)WS_3\}_2Hg]$ (**17**) with 50% thermal ellipsoids. Hydrogen atoms are omitted for clarity. Reproduced with permission from Ref. [58].

### 4.4. $M_2M'$-type clusters

Only one compound is known: $[\{(\eta^5\text{-}C_5Me_5)WS_3\}_2\text{-}Hg]$ (**17**) [58]. Reaction of **1** with 0.5 equiv. of $HgCl_2$ in DMF formed thin brown crystals of **17** in a relatively high yield. As depicted in Fig. 15, the neutral cluster consists of a slightly bent linear structure (S(1)–Hg–S(1*) bond angle = 174.6(3)°) in which each of the two $[(\eta^5\text{-}C_5Me_5)WS_3]^-$ species act as monodentate ligand to bind the central Hg via one S atom. Such a coordination (fragment **d**) is unprecedented in thiometallate chemistry. The Hg–S bond length of 2.31 Å is 0.29 Å shorter than that in $[(WS_4)_2Hg]^{2-}$ (2.603 Å) [21] while the W–S(1)–Hg angle of 93.2° is remarkably larger than that in $[(WS_4)_2Hg]^{2-}$ (78.7°). In the trinuclear complexes $[(MS_4)_2M']^{z-}$ ($z = 2$, M = Mo, W; M′ = Ni [78,79], Mn [80], Fe [81–83], Rh [84], Pd [85], Zn [86], Hg [21]; $z = 3$, M = Mo, W; M′ = Fe [21], Cu [21], Ag [21], Co [87,88]), the central M′ is surrounded by four doubly bridging sulfur atoms belonging in pairs to two $MS_4$ fragments; the geometry of the M′ atom adopts either a distorted tetrahedral or a square-planar geometry ($d^8$ metal ions such as $Ni^{2+}$, $Pd^{2+}$).

### 4.5. $M_2M'_3$-type clusters

The only compound $[\{(\eta^5\text{-}C_5Me_5)WS_3\}_2Ag_3(PPh_3)_3](NO_3)$ (**18**) was prepared through the reaction of **1** with $[Ag(PPh_3)_2(NO_3)]$ in MeCN [52]. As shown in Fig. 16, the structure of the cation of **18** may be regarded as a composite of one $[(\eta^5\text{-}C_5Me_5)WS_3Ag]$ fragment (**a**) and one $[(\eta^5\text{-}C_5Me_5)WS_3Ag_2]$ fragment (**b**), which are connected in a complicated way through Ag–S interactions. The A(1) and Ag(2a) atoms show a strongly distorted tetrahedral coordination geometry, while the Ag(3) adopts a pyramidalized Y shape coordination geometry, though we noticed the presence of a weak Ag(3) and S(3) interaction (2.89 Å). The inter-fragment Ag–S lengths vary from Ag(2a)–S(1) = 2.663(3) Å to Ag(1)–S(6) = 2.715(2) Å, while the Ag–S lengths within each fragment range from 2.503(3) to 2.664(3) Å. The W–Ag lengths, ranging from 3.016(1) to 3.18 Å, are longer than those of **9**. Interestingly, these inter-fragment Ag–S interactions bind the two fragments tightly, and they are not dissociated easily even in acetonitrile solution according to the ESI-MS analysis [52].

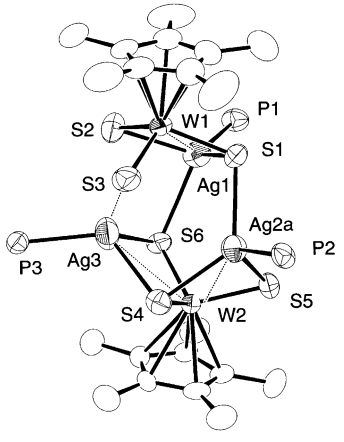


Fig. 16. Structure of the cation of $[\{(\eta^5\text{-}C_5Me_5)WS_3\}_2Ag_3(PPh_3)_3](NO_3)$ (**18**) with 50% thermal ellipsoids. Only one of the distorted Ag(2) atom, i.e. Ag(2a), is shown, that was refined with site occupancy factor of 0.85, and phenyl groups and hydrogen atoms are omitted for clarity. Reproduced with permission from Ref. [52].

### 4.6. $M_2M'_6$-type clusters

Four clusters $[PPh_4]_2[(\eta^5\text{-}C_5Me_5)MS_3(CuX)_3]_2$ (**19**: M = Mo, X = Br; **20**: M = W, X = Cl; **21**: M = W, X = Br; **22**: M = W, X = SCN) have been synthesized. Octanuclear clusters **19**–**22** were obtained from the reactions of **1** or **2** with 3 equiv. of CuX (X = Cl, Br, SCN) in MeCN [48,53] in almost quantitative yield.

Although **19**–**21** are isomorphous, only the structure of the dianion of **19** is shown in Fig. 17. Compound **19** contains two incomplete $(\eta^5\text{-}C_5Me_5)MoS_3Cu_3$ fragments (**c**), which are interconnected by a couple of weak Cu–Br–Cu bridges. There is a crystallographic inversion center located at the center of the dianion. The Cu(1) atom adopts a distorted tetrahedral geometry while the Cu(2) and Cu(3) atoms are trigonal-planar. Therefore, the Mo–Cu(1) length (2.660(1) Å) is slightly longer than those of the Mo(2) and Mo–Cu(3) lengths (2.652(2) and 2.644(2) Å). Within the $CuBr_2Cu$ ring, the Cu(1)–Br(1*) and Cu(1*)–Br(1) lengths (2.919(4) Å) are significantly longer than the Cu(1)–Br(1) and Cu(1*)–Br(1*) bonds (2.345(1) Å). The same phenomenon is also observed for **20** and **21**.

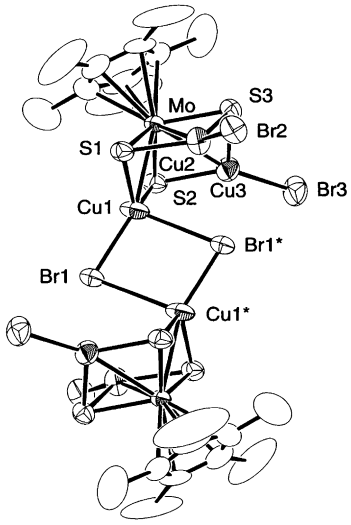


Fig. 17. Structure of the dianion of $[PPh_4]_2[(\eta^5\text{-}C_5Me_5)MoS_3(CuBr)_3]_2$ (**19**) with 50% thermal ellipsoids. Hydrogen atoms are omitted for clarity. Reproduced with permission from Ref. [53].

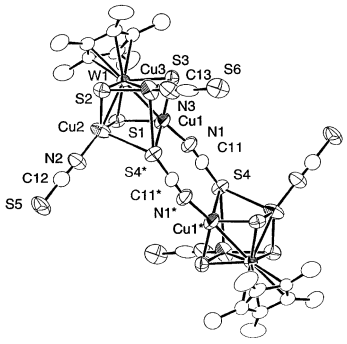


Fig. 18. Structure of the dianion of $[PPh_4]_2[(\eta^5\text{-}C_5Me_5)WS_3(CuNCS)_3]_2$ (**22**) with 50% thermal ellipsoids. Hydrogen atoms are omitted for clarity. Reproduced with permission from Ref. [48].

On the other hand, two incomplete $(\eta^5\text{-}C_5Me_5)WS_3Cu_3$ fragments (**c**) in the structure of **22** are linked via interactions between the sulfur end of one NCS ligand in each fragment and three copper atoms of the other fragment (Fig. 18). Thus like the triply-bridging Cl in **15**, the NCS sulfur fills a void of the $WS_3Cu_3$ incomplete cubane. The occurrence of triply-bridging NCS sulfur is unprecedented, although double bridging was observed in the polymeric structures of $[PyH][Cu_2(NCS)_3]$ [89] and $[NEt_4]_3[WS_4Cu_4(NCS)_5]$ [90]. The eight-membered Cu(1)N(1)C(11)S(4)Cu(1*)N(1*)C(11*)S(4*) ring is nearly planar. The coordination geometry at each copper atom is ca. trigonal-planar, to which an NCS sulfur is weakly bound from the direction perpendicular to the plane. The mean Cu–S(SCN) distance of 2.952(4) Å is remarkably longer than other Cu–S distances (average value = 2.230(2) Å). The mean W–Cu length is 2.652(2) Å, which resembles those containing three-coordinated Cu clusters in **11**, **13**, and **16**.

An important feature for **19**–**22** is that both Cu–Br–Cu and Cu–NCS–Cu bridges are weak, and they may be cleaved easily in a donor solvent and/or in the presence of strong donor ligands. In fact, only the monoanion $[(\eta^5\text{-}C_5Me_5)WS_3(CuX)_3]^-$ was detected in MeCN by ESI-MS experiments. Thus dissociation of $[(\eta^5\text{-}C_5Me_5)WS_3(CuX)_3]_2^{2-}$ may precede the reactions with $AsPh_3$, $PPh_3$ and dppm in MeCN. The observed ESI-MS spectrum of **19** with the calculated isotopic distributions for $[(\eta^5\text{-}C_5Me_5)MoS_3(CuX)_3]^-$ and $[(\eta^5\text{-}C_5Me_5)MoS_3(CuX)_3]_2^{2-}$ are displayed in Fig. 19.

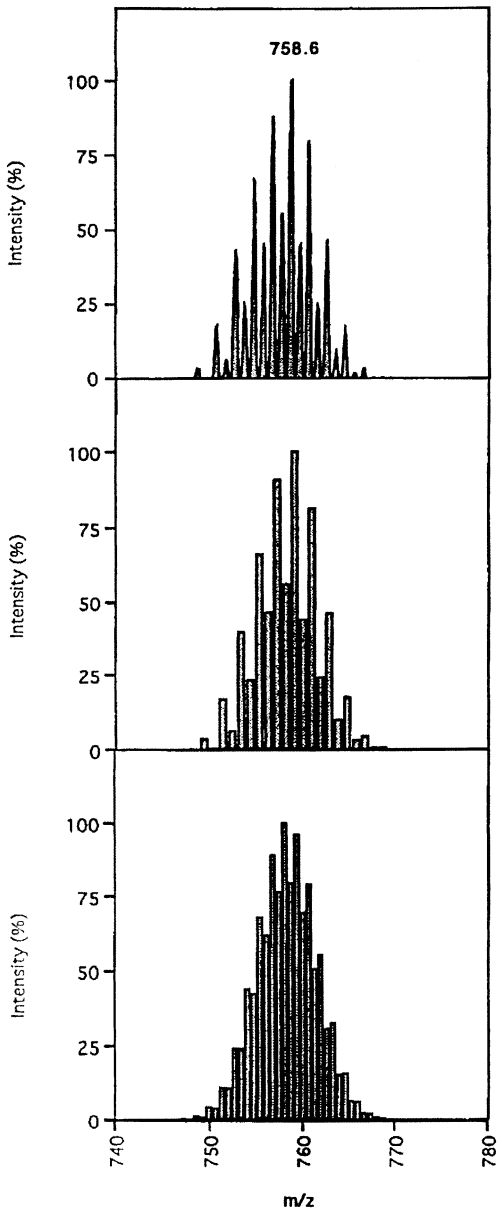


Fig. 19. Comparison between the observed ESI-MS for **19** (a) and the calculated isotopic distributions for $[(\eta^5\text{-}C_5Me_5)MoS_3(CuBr)_3]^-$ (b) and $[(\eta^5\text{-}C_5Me_5)MoS_3(CuBr)_3]_2^{2-}$ (c). Reproduced with permission from Ref. [53].

### 4.7. $M_3M'_6$-type clusters

Compound $[PPh_4][\{(\eta^5\text{-}C_5Me_5)WS_3Cu_2\}_3S_2]$ (**23**) was obtained from the reaction of **21** with excess $Li_2S_2$ in MeCN [51]. The structure of the anion of **23** can be described as three chemically equivalent $[(\eta^5\text{-}C_5Me_5)WS_3Cu_2]$ cluster fragments (**b**) interconnected by two triply bridging $S^{2-}$ ligands (Fig. 20). Alternatively, the main frame of the structure may be viewed as a face bicapped trigonal prism made by six copper atoms and two sulfur atoms, and each of the three non-bonded Cu···Cu edges is bound to one $(\eta^5\text{-}C_5Me_5)WS_3$ moiety. This core structure resembles that of $[NEt_4]_4[(WSe_4Cu_2)_3Se_2]$ [91], in which three $[WSe_4]^{2-}$ moieties bridge two $Cu_3$ triangles. One $Cu_3$ (Cu(1), Cu(4), Cu(5)) triangular plane is nearly parallel (1.4°) to the opposite $Cu_3$ (Cu(2), Cu(3), Cu(6)) plane. The Cu···Cu distances within the trigonal planes range from 2.91 to 3.06 Å, while those connecting the planes are somewhat longer, being 3.11–3.18 Å. The two sulfur

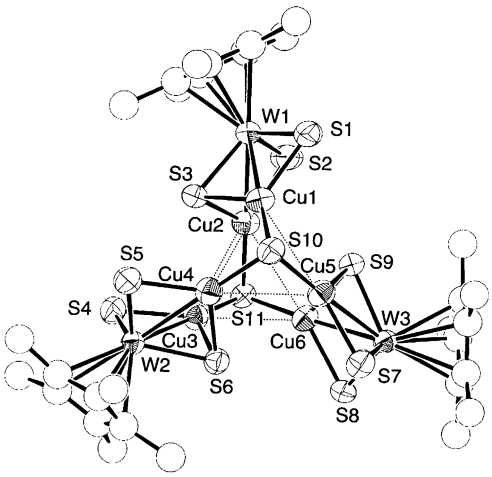


Fig. 20. Structure of the anion of $[PPh_4][\{(\eta^5\text{-}C_5Me_5)WS_3Cu_2\}_3S_2]$ (**23**) with 50% thermal ellipsoids. Hydrogen atoms are omitted for clarity. Reproduced with permission from Ref. [51].

atoms, S(10) and S(11), sit 1.37 Å above (or below) the corresponding triangular $Cu_3$ planes. The dihedral angles between the $S_3$ planes of the three $(\eta^5\text{-}C_5Me_5)WS_3$ moieties are all close to 60°, implying the core possesses an approximate 3-fold symmetry, and the pseudo $C_3$ axis runs through S(10) and S(11). Each Cu adopts a trigonal-planar coordination geometry with three sulfur atoms of different types. The W–Cu distances of 2.665(2)–2.683(2) Å are also short, and are comparable to those observed in **20**–**22**.

### 4.8. $M_3M'_7$-type clusters

Compound $[\{(\eta^5\text{-}C_5Me_5)WS_3\}_3Cu_7(MeCN)_9](PF_6)_4$ (**24**) was isolated from the reaction of **1** with 3 equiv. of $[Cu(MeCN)_4](PF_6)$ in MeCN [56]. The tetracationic cluster $[\{(\eta^5\text{-}C_5Me_5)WS_3\}_3Cu_7(MeCN)_9]^{4+}$ contains three $(\eta^5\text{-}C_5Me_5)WS_3$ moieties linked by two copper atoms Cu(3) and Cu(5), five more copper atoms chelate the sulfur ends to form a $W_3Cu_7S_9$ core (Fig. 21). Alternatively, the core structure of **24** can be viewed as built up via three corner-shared triply-fused incomplete $(\eta^5\text{-}C_5Me_5)WS_3Cu_3$ fragments (**c**). While the bridging copper atoms are tetrahedrally surrounded by four sulfur atoms, a total of nine MeCN molecules further coordinate to the latter five copper atoms to complete their coordination geometries. Interestingly, the cluster structure is asymmetric in that Cu(2) coordinates only one MeCN molecule while each of the other copper atoms coordinates two MeCN molecules. It is rather surprising that one copper, Cu(2), assumes a trigonal-planar coordination geometry with N(MeCN) and $\mu_3$-S atoms, despite the fact that the cluster was synthesized and recrystallized using MeCN as a solvent. The W–Cu distances of **24** can be classified into three groups: a short W(1)–Cu(2) bond of 2.620(3) Å, long W–Cu(3,5) bonds of 2.759(3)–2.779(3) Å, and the remaining W–Cu bonds with intermediate distances of 2.695(3)–2.720(4) Å. The observed trend of W–Cu bond lengths correlates with the number of bonding interactions at the Cu centers. The long W–Cu distances occur at Cu atoms, Cu(3) and Cu(5), each of which interacts with four S atoms and two W atoms, while the short W–Cu distance is observed for Cu(2) which interacts with three ligands and one W atom.

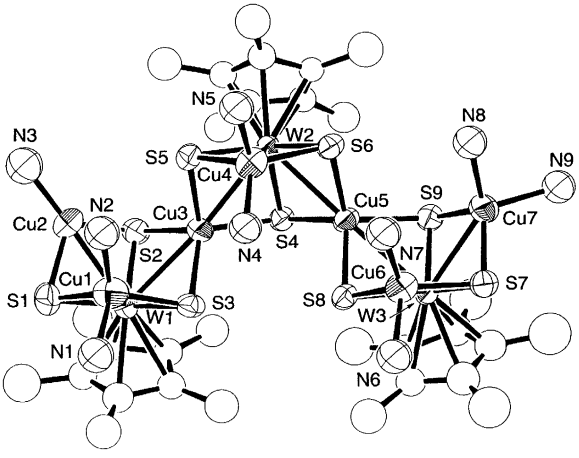


Fig. 21. Structure of the tetracation of $[\{(\eta^5\text{-}C_5Me_5)WS_3\}_3\text{-}Cu_7(CH_3CN)_9](PF_6)_4$ (**24**) with 50% thermal ellipsoids. For clarity, hydrogen atoms are omitted, and the MeCN molecules coordinated at the Cu atoms are represented by the pivotal N atoms. Reproduced with permission from Ref. [56].

### 4.9. $M_4M'_4$-type clusters

Only two clusters were isolated: $[(\eta^5\text{-}C_5Me_5)WS_3M']_4$ (**25**: M′ = Cu [55]; **26**: M′ = Ag [54]). The former was separated from reaction of **1** with equimolar CuBr in $CHCl_3$ while the latter was obtained from reaction of **1** with equimolar $[Ag(MeCN)_4](PF_6)$ in MeCN. As shown

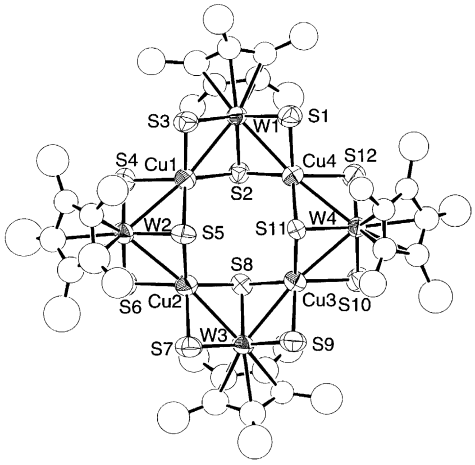


Fig. 22. Molecular structure of $[(\eta^5\text{-}C_5Me_5)WS_3Cu]_4$ (**25**) with 50% thermal ellipsoids. Hydrogen atoms are omitted for clarity. Reproduced with permission from Ref. [55].

in Fig. 22, X-ray analysis of **25** revealed that four corner-shared [($\eta^5$-$C_5Me_5$)$WS_3Cu_2$] cluster fragments (**b**) are quadruply-fused into a 'four-flier pin-wheel' structure with an approximate $S_4$ symmetry. The $W_4Cu_4$ core structure resembles those of $[NEt_4]_4[MOS_3Cu]_4$ (M = Mo, W) [92], in which four $[MOS_3]^{2-}$ moieties are linked by four copper atoms via S bridges. Within the $W_4Cu_4$ cluster core, the four W and the four Cu atoms are nearly coplanar, with the maximum deviation from the least-squares plane being 0.3 Å. Each Cu atom moves inward from the midpoint of each edge of the $W_4$ square, and the average W–Cu–W angle is 172°. The ($\eta^5$-$C_5Me_5$)$WS_3$ moieties are situated alternatively above and below the $W_4Cu_4$ mean plane, and so are the bridging sulfur atoms. Each Cu is tetrahedrally coordinated by four S atoms. The mean W–Cu length of 2.751(3) Å is similar to that of $[NEt_4]_4[WOS_3Cu]_4$ (2.747 Å) [92].

On the other hand, the molecular structure of **25** is constructed of four [($\eta^5$-$C_5Me_5$)$WS_3Ag$] cluster fragments (**a**) connected in a head-to-end manner (Fig. 23). Although the $W_4Ag_4$ core structure of **26** roughly resembles that of the $W_4Cu_4$ core in **24**, it has some other interesting structural features not evident in its copper analogue. In **25**, one W=S bond of the ($\eta^5$-$C_5Me_5$)$WS_3$ moiety remains intact, and the coordination geometry at Ag is a slightly pyramidalized Y-shape. The W–Ag distance of 2.948(2) Å, comparable to that of **8**, is substantially shorter than the W–Ag* length of 3.266(3) Å.

## 5. Concluding remarks

In this article we have reported the synthesis of a relatively young family of new heterobimetallic sulfide clusters containing [$PPh_4$][($\eta^5$-$C_5Me_5$)$MS_3$] (**1**: M = W; **2**: M = Mo). A range of unusual structures including a 1D ladder-like chain, a 1D helical chain, a 2D network, and a corner-shared triply-fused incomplete cubane cluster framework have been presented. These unusual structures demonstrate that **1** and **2** can be used as versatile building blocks in the assembly of interesting heterometallic sulfide clusters. These mononuclear metal sulfide ligands complement and extend the chemistry of their homoleptic congeners such as $[MS_4]^{2-}$ (M = Mo, W). We are currently developing the chemistry reported here in the pursuit of materials with good third-order non-linear optical properties and in an endeavor to model the FeMoco structure in nitrogenases.

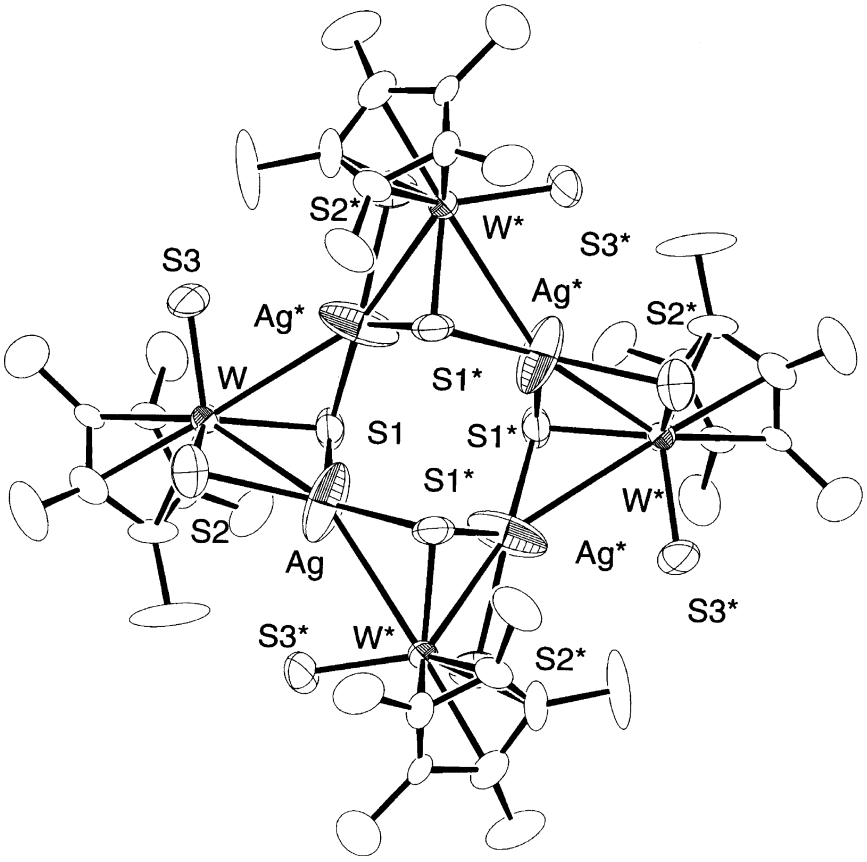


Fig. 23. Molecular structure of [($\eta^5$-$C_5Me_5$)$WS_3Ag$]$_4$ (**26**) with 50% thermal ellipsoids. Hydrogen atoms are omitted for clarity. Reproduced with permission from Ref. [54].

## Acknowledgements

The authors would like to thank Professor Hiroyuki Kawaguchi of Institute of Molecular Science in Japan and Professor Roger. E. Cramer of Hawaii University for their helpful comments. The work was partially supported by the Key Laboratory of Organic Chemistry of Jiangsu Province at Suzhou University (No. KJS01017) and the National Natural Science Foundation in China (No. 20271036).

## References

[1] P. Braunstein, L.A. Oro, P.R. Raithby (Eds.), Metal Clusters in Chemistry, vol. 1–3, Wiley-VCH, New York, 1999.
[2] R.D. Adams, F.A. Cotton (Eds.), Catalysis by Di- and Polynuclear Metal Cluster Complexes, Wiley-VCH, New York, 1998.
[3] B. Krebs, G. Henkel, Angew. Chem. Int. Ed. Engl. 30 (1991) 769.
[4] L.C. Roof, J.W. Kolis, Chem. Rev. 93 (1993) 1037.
[5] T. Saito, in: M.H. Chisholm (Ed.), Early Transition Metal Clusters with p-Donor Ligands, VCH, New York, 1995, pp. 63–164.
[6] D. Fenske, N.-Y. Zhu, T. Langetepe, Angew. Chem. Int. Ed. Engl. 37 (1998) 2639.
[7] G. Parkin, Prog. Inorg. Chem. 47 (1998) 1.
[8] I. Dance, Prog. Inorg. Chem. 41 (1994) 637.
[9] M.R. Dubois, Chem. Rev. 89 (1989) 1.
[10] M. Hidai, S. Kuwata, Y. Mizobe, Acc. Chem. Res. 33 (2000) 46.
[11] R.H. Holm, Adv. Inorg. Chem. 38 (1992) 1.
[12] R. Hernandez-Molina, A.G. Sykes, J. Chem. Soc. Dalton Trans. (1999) 3137.
[13] A.S.A. Tor, J. Cluster Sci. 7 (1996) 263.
[14] M.G. Kanatzidis, A.C. Sutorik, Prog. Inorg. Chem. 43 (1995) 151.
[15] P. Boorman, X.-L. Gao, H.B. Kraatz, V. Mozol, M.-P. Wang, in: E.I. Stiefel, K. Matsumoto (Eds.), Transition Metal Sulfur Chemistry, Biological and Industrial Significance, ACS Symposium Series 653, American Chemical Society, Washington, DC, 1996, pp. 197–214.
[16] A. Müller, E. Diemann, R. Jostes, H. Bögge, Angew. Chem. Int. Ed. Engl. 20 (1981) 934.
[17] G. Christou, C.D. Garner, F.E. Mabbs, T.J. King, J. Chem. Soc. Chem. Commun. (1978) 740.
[18] Y. Jeannin, F. Sécheresse, S. Bernes, F. Robert, Inorg. Chim. Acta 198–200 (1992) 493.
[19] D. Coucouvanis, Adv. Inorg. Chem. 104 (1998) 682.
[20] K.E. Howard, T.B. Rauchfuss, A.L. Rheingold, J. Am. Chem. Soc. 108 (1986) 297.
[21] A. Müller, H. Bögge, U. Schimanski, M. Penk, K. Nieradzik, M. Dartmann, E. Krickemeyer, J. Schimanski, C. Römer, M. Römer, H. Dornfeld, U. Wienböker, W. Hellmann, Monatsh Chem. 120 (1989) 367.
[22] R.H. Holm, Pure Appl. Chem. 67 (1995) 2117.
[23] T. Shibahara, Coord. Chem. Rev. 123 (1993) 73.
[24] M.A. Ansari, J.A. Ibers, Coord. Chem. Rev. 100 (1990) 223.
[25] H.-W. Hou, X.-Q. Xin, S. Shi, Coord. Chem. Rev. 153 (1996) 25.
[26] X.T. Wu, P.C. Chen, S.W. Du, N.Y. Zhu, J.X. Lu, J. Cluster Sci. 5 (1994) 265.
[27] E.I. Stiefel, D. Coucouvanis, W.E. Newton (Eds.), Molybdenum Enzymes, Cofactors and Model Systems, ACS Symposium Series 535, American Chemical Society, Washington, DC, 1993.
[28] C.F. Mills, Philos. Trans. R. Soc. London Ser. B 288 (1979) 51.
[29] P.A. Eldredge, B.A. Averill, J. Cluster Sci. 1 (1990) 269.
[30] R.H. Holm, Adv. Inorg. Chem. 38 (1992) 1.
[31] R.R. Eady, G.J. Leigh, J. Chem. Soc. Dalton Trans. (1994) 2739.
[32] E.I. Stiefel, K. Matsumoto (Eds.), Transition Metal Sulfur Chemistry, Biological and Industrial Significance, ACS Symposium Series 653, American Chemical Society, Washington, DC, 1996.
[33] R.R. Chianelli, T.A. Picoraro, T.R. Halbert, W.H. Pan, E.I. Stiefel, J. Catal. 86 (1984) 226.
[34] T.B. Rauchfuss, Prog. Inorg. Chem. 39 (1991) 259.
[35] M.D. Curtis, Appl. Organomet. Chem. 6 (1992) 429.
[36] A. Müller, E. Diemann, A. Branding, F.W. Baumann, Appl. Catal. 62 (1990) L13.
[37] M.D. Curtis, J. Cluster Sci. 7 (1996) 247.
[38] S. Shi, W. Ji, S.-H. Tang, J.-P. Lang, X.-Q. Xin, J. Am. Chem. Soc. 116 (1994) 3615.
[39] J.-P. Lang, K. Tatsumi, H. Kawaguchi, J.-M. Lu, P. Ge, W. Ji, S. Shi, Inorg. Chem. 35 (1996) 7924.
[40] S. Shi, in: D.M. Roundhill, J.P. Fackler, Jr. (Eds.), Optoelectronic Properties of Inorganic Compounds, Plenum Press, New York, 1998, pp. 55–105.
[41] C. Zhang, Y.-L. Song, B.-M. Fung, Z.-L. Xue, X.-Q. Xin, Chem. Commun. (2000) 843.
[42] H. Yu, Q.-F. Xu, Z.-R. Sun, Q. Liu, J.-X. Chen, S.-J. Ji, J.-P. Lang, K. Tatsumi, Chem. Commun. (2001) 2614.
[43] K. Tatsumi, Y. Inoue, A. Nakamura, R.E. Cramer, W. VanDoorne, J.W. Gilje, J. Am. Chem. Soc. 111 (1989) 782.
[44] K. Tatsumi, Y. Inoue, H. Kawaguchi, M. Kohsaka, A. Nakamura, R.E. Cramer, W. Van Doorne, G.J. Taogoshi, P.N. Richmann, Organometallics 12 (1993) 352.
[45] H. Kawaguchi, K. Tatsumi, J. Am. Chem. Soc. 117 (1995) 3885.
[46] H. Kawaguchi, K. Yamada, J.-P. Lang, K. Tatsumi, J. Am. Chem. Soc. 119 (1997) 10346.
[47] K. Tatsumi, H. Kawaguchi, Y. Inoue, A. Nakamura, R.E. Cramer, J.A. Golen, Angew. Chem. Int. Ed. Engl. 32 (1993) 32.
[48] J.-P. Lang, H. Kawaguchi, S. Ohnishi, K. Tatsumi, J. Chem. Soc., Chem. Commun. (1997) 405.
[49] J.-P. Lang, H. Kawaguchi, K. Tatsumi, Inorg. Chem. 36 (1997) 6447.
[50] K. Tatsumi, J.-P. Lang, S. Ohnishi, T. Nagasawa, H. Kawaguchi, J. Inorg. Biochem. 67 (1997) 269.
[51] J.-P. Lang, K. Tatsumi, Inorg. Chem. 37 (1998) 160.
[52] J.-P. Lang, H. Kawaguchi, K. Tatsumi, J. Organomet. Chem. 569 (1998) 109.
[53] J.-P. Lang, H. Kawaguchi, S. Ohnishi, K. Tatsumi, Inorg. Chim. Acta 283 (1998) 136.
[54] J.-P. Lang, K. Tatsumi, Inorg. Chem. 38 (1999) 1364.
[55] J.-P. Lang, K. Tatsumi, J. Organomet. Chem. 579 (1999) 332.
[56] J.-P. Lang, H. Kawaguchi, K. Tatsumi, Chem. Commun. (1999) 2315.
[57] M.S. Rau, C.M. Kretz, G.L. Geoffroy, A.L. Rheingold, Organometallics 12 (1993) 3447.
[58] J.-P. Lang, K. Tatsumi, unpublished results.
[59] F. Canales, M.C. Gimeno, P.G. Jones, A. Laguna, J. Chem. Soc. Dalton Trans. (1997) 439.
[60] J.C. Huffmann, R.S. Roth, A.R. Siedle, J. Am. Chem. Soc. 98 (1976) 4340.
[61] B. Wu, W.-J. Zheng, X.-Y. Huang, X.-T. Wu, S.-Y. Yu, Polyhedron 16 (1997) 801.
[62] K.E. Howard, T.B. Rauchfuss, S.R. Wilson, Inorg. Chem. 27 (1988) 3561.
[63] R. Cao, X.-J. Lei, M.-C. Huang, Z.-Y. Huang, H.-Q. Liu, Chin. J. Struct. Chem. 11 (1992) 34.
[64] S.-W. Du, N.-Y. Zhu, P.-C. Chen, X.-T. Wu, Polyhedron 11 (1992) 2489.
[65] A. Müller, U. Schimanski, J. Schimanski, Inorg. Chim. Acta 76 (1983) L245.

[66] J.-P. Lang, H.-Z. Zhu, X.-Q. Xin, M.-Q. Chen, K. Liu, P.-J. Zheng, Chin. J. Chem. 11 (1993) 21.
[67] J.-P. Lang, H.-Z. Zhu, X.-Q. Xin, K.-B. Yu, Chin. J. Struct. Chem. 11 (1992) 27.
[68] J.P. Fackler, Jr., C.A. Lopez, R.J. Staples, S. Wang, R.E.P. Winpenney, R.P. Lattimer, J. Chem. Soc. Chem. Commun. (1992) 146.
[69] E. Block, M. Gernon, H. Kang, G. Ofori-Okai, J. Zubieta, Inorg. Chem. 28 (1989) 1263.
[70] Q. Huang, X.-T. Wu, Q.-M. Wang, S.-L. Sheng, J.-X. Lu, Angew. Chem. Int. Ed. Engl. 35 (1996) 868.
[71] J.-P. Lang, J.-G. Li, S.-A. Bao, X.-Q. Xin, Polyhedron 12 (1993) 801.
[72] A. Müller, H. Bögge, E. Königer-Ahlborn, W. Hellmann, Inorg. Chem. 18 (1979) 2301.
[73] A. Müller, H. Bögge, E. Königer-Ahlborn, J. Chem. Soc. Chem. Commun. (1979) 739.
[74] P. Braunstein, B. Oswald, A. Tripicchio, M.T. Camellini, Angew Chem. Int. Ed. Engl. 29 (1990) 1140.
[75] J.D. Graybeal, G.L. Mckown, Inorg. Chem. 5 (1966) 1909.
[76] Z.-R. Chen, H.-W. Hou, X.-Q. Xin, K.-B. Yu, S. Shi, J. Phys. Chem. 99 (1995) 8717.
[77] A. Müller, H. Bögge, U. Schimanski, Inorg. Chim. Acta 69 (1983) 5.
[78] A. Müller, E. Diemann, J. Chem. Soc. Chem. Commun. (1971) 65.
[79] A. Bencini, F. Cecconi, C.A. Ghilardi, S. Midollini, F. Nuzzi, A. Orlandini, Inorg. Chem. 31 (1992) 5339.
[80] G. Sánchez, F. Momblona, G. García, G. López, E. Pinilla, A. Monge, J. Chem. Soc. Dalton Trans. (1994) 2271.
[81] D. Coucouvanis, N.C. Baenziger, E.D. Simhon, P. Stremple, D. Swenson, A. Simopoulos, A. Kostikas, V. Petrouleas, V. Papaefthymiou, J. Am. Chem. Soc. 102 (1980) 1732.
[82] D. Coucouvanis, Acc. Chem. Res. 14 (1981) 201.
[83] D. Coucouvanis, E.D. Simhon, P. Stremple, M. Ryan, D. Swenson, N.C. Baenziger, A. Simopoulos, V. Papaefthymiou, A. Kostikas, V. Petrouleas, Inorg. Chem. 23 (1984) 741.
[84] K.E. Howard, T.B. Rauchfuss, A.L. Rheingold, J. Am. Chem. Soc. 108 (1986) 297.
[85] K.E. Howard, T.B. Rauchfuss, S.R. Wilson, Inorg. Chem. 27 (1988) 3561.
[86] I. Paulat-Böschen, B. Krebs, A. Müller, E. Königer-Ahlborn, H. Dornfeld, H. Schulz, Inorg. Chem. 17 (1978) 1440.
[87] A. Müller, W. Hellmann, J. Schneider, U. Schimanski, U. Demmer, A. Trautwein, W. Hellmann, Inorg. Chim. Acta 65 (1982) L41.
[88] W.-H. Pan, D.C. Johnston, S.T. McKenna, R.R. Chianelli, T.R. Halbert, L.L. Hutchings, E.I. Stiefel, Inorg. Chim. Acta 97 (1997) L17.
[89] C.L. Raston, B. Walter, A.H. White, Aust. J. Chem. 32 (1979) 2757.
[90] J.M. Manoli, C. Potvin, F. Sécheresse, S. Marzak, Inorg. Chim. Acta 150 (1988) 259.
[91] C.C. Christuk, M.A. Ansari, J.A. Ibers, Angew. Chem. Int. Ed. Engl. 31 (1992) 1477.
[92] Q. Huang, X.-T. Wu, Q.-M. Wang, T.-L. Sheng, J.-X. Lu, Inorg. Chem. 35 (1996) 893.